Effect of Spatial Filtering on Crosstalk Reduction in Surface EMG Recordings

Medical Engineering & Physics

Effect of Spatial Filtering on Crosstalk Reduction in Surface EMG Recordings

Luca Mesin[1*], Stuart Smith[2], Suzanne Hugo[2], Suretha Viljoen[2], Tania Hanekom[2]

[1] *Laboratorio di Ingegneria del Sistema Neuromuscolare (LISiN), Dipartimento di Elettronica, Politecnico di Torino, Torino, Italy*

[2] *Department of Electrical, Electronic and Computer Engineering, University of Pretoria, Pretoria, South Africa*

Keywords: electromyography, surface EMG modelling, crosstalk, spatial filters

Running title: Spatial filtering for crosstalk reduction

Address for correspondence:
* Luca Mesin, Ph.D.
Dipartimento di Elettronica, Politecnico di Torino
Corso Duca degli Abruzzi 24, Torino, 10129 ITALY
Tel. 0039-011-4330476; Fax. 0039-0114330404; e-mail: luca.mesin@ polito.it

ABSTRACT

Increasing the selectivity of the detection system in surface electromyography (EMG) is beneficial in the collection of information of a specific portion of the investigated muscle and to reduce the contribution of undesired components, such as non-propagating components (due to generation or end-of-fibre effects) or crosstalk from nearby muscles. A comparison of the ability of different spatial filters to reduce the amount of crosstalk in surface EMG measurements was conducted in this paper using simulated signals. It focused on the influence of different properties of the muscle anatomy (changing subcutaneous layer thickness, skin conductivity, fibre length) and detection system (single, double and normal double differential, with two interelectrode distances - IED) on the amount of crosstalk present in the measurements. A cylindrical multilayer (skin, subcutaneous tissue, muscle, bone) analytical model was used to simulate single fibre action potentials (SFAPs). Fibres were grouped together in motor units (MU) and motor unit action potentials (MUAP) were obtained by adding the SFAPs of the corresponding fibres. Interference surface electromyogram (EMG) signals were obtained, modelling the recruitment of MUs and rate coding. The average rectified value (ARV) and mean frequency content (MNF) of the EMG signals were studied and used as a basis for determining the selectivity of each spatial filter. From these results it was found that the selectivity of each spatial filter varies depending on the transversal location of the measurement electrodes and on the anatomy. An increase in skin conductivity favourably affects the selectivity of normal double differential filters as does an increase in subcutaneous layer thickness. An increase in IED decreases the selectivity of all the analyzed filters.

INTRODUCTION

Crosstalk is one of the main issues in surface electromyography (EMG) recordings [1-3]. It is the signal recorded over one muscle that is actually generated by a nearby muscle and conducted through the volume conductor to the recording electrodes [4-6]. Many previous studies have investigated crosstalk experimentally [1,2,4,6-9] and by mathematical simulations [1,3,7,10-12].

It has been shown that far-field potentials, mainly contributing to crosstalk signals, are due to the extinction of the intracellular action potential at the fibre endings (the so-called end-of-fibre components) [1,5,7,13,14]. As a consequence, crosstalk signals may not have a smaller bandwidth than signals detected directly over the active muscle, as was hypothesized in the past [15].

Moreover, signals generated by the same muscle and detected close and far from such a muscle may be poorly correlated [1,11], thus methods based on the cross-correlation analysis of EMG signals, suggested in the past for identifying crosstalk [6,9], have not been effective [1] .

Crosstalk depends on many anatomical and physical factors of the surface EMG generation system [1,11,12,17]. Subcutaneous layer thickness increases crosstalk, as proven experimentally [18] and by simulations [17]. Furthermore, the conductivity of the skin [11,17] as well as the occurrence of a superficial bone influence crosstalk [19,20]. In addition, the electrode system used to record the signal significantly affects the amount of crosstalk [1,21].

Surface EMG signals can be detected by a number of spatial filters, the bipolar system [4,22] being the most common. Spatial filters perform the linear combination of the signals detected by electrodes located in a specific one-dimensional (1-D) or two-dimensional (2-D) configuration. The selectivity of a spatial filter is described by its spatial transfer function [23], which can be derived by the 2-D Fourier transform of the filter impulse response (the filter mask).

The transfer function characterizes the effect of the spatial filter on signal components that travel along the direction of the muscle fibre. For signal components that do not travel in a specific direction, such as the end-of-fibre components [13], the effect of the surface EMG detection system cannot be described in terms of the spatial filter transfer function [24-26]. The analytical prediction of the effect of the detection system on far-field potentials is thus complex. Modelling studies have shown that high-pass spatial filters which show high selectivity for the propagating signal components may not be as selective for the non-propagating components [1,24,26]. Moreover, it has been shown that the effect of a spatial filter on the end-of-fibre components also depends on the volume conductor properties [27].

When practical measures are considered, crosstalk may be due to a combination of travelling and non-travelling signal components depending on the distance of the active muscle fibres from the detection point. Past modelling studies, which compared the effect of the detection system on crosstalk, focused on single fibre [27] or single MU [3,10] action potential simulation. Although these studies provided an important basis for interpreting experimental recordings, a closer approximation of experimental conditions could be provided by the simulation of interference surface EMG signals that are generated by many MUs controlled with a specific strategy.

Additionally, the simulation of the activity of all the fibres in a muscle implies that the sources are at different distances from the detection points, thus their contribution to crosstalk may be different. The contribution to the EMG signal of some fibres may be mainly attributed to the travelling components or the end-of-fibre signals originating from those fibres, thus the detection spatial filter will have a different selectivity with respect to the various sources contributing to the interference signal. Predicting the effect of the detection system on crosstalk in such conditions is not possible analytically but requires a numerical approach. A previous simulation study on crosstalk analyzed interference surface EMG signals [11] but limited the analysis to one-dimensional (1-D) spatial filters.

The aim of this study was to analyze the effect of 1-D and 2-D detection systems on crosstalk reduction by realistic simulations of the interference EMG signal. For this purpose, a mathematical description of the muscle fibre anatomy and of the MU control strategies was used.

METHODS

Volume conductor model

The analytical model developed in [28] was used to generate SFAPs. The model describes a cylindrical layered volume conductor with bone, muscle, subcutaneous, and skin tissues [1,17]. A specific part of the muscle region comprises the active muscle fibres. The active muscle territory was described as an ellipse, specified by its centre and two semi-axes. The parameters that were fixed in the volume conductor model are reported in Table 1.

Table 1 about here

To reduce computational cost, a low density of fibres was simulated. It corresponded to the fibre density in the MUs, which is about 10 times lower than fibre density in a muscle [29]. Subcutaneous layer thickness, skin layer conductivity and fibre length varied across simulations, as reported in Table 2. Thicknesses of tissues were chosen to compare the case of a thin and a fat subject. The value of conductivity of skin varied between the maximum value used in [27] and the measured conductivity reported in [30]. Libraries of 12,000 SFAPs (600 mm^2 cross-sectional area with 20 fibres/mm^2 fibre density) were simulated for each anatomical condition.

Table 2 about here

Detection system

The simulated spatial filters were single differential (SD), double differential (DD) and Laplacian or normal double differential (NDD), with inter-electrode distances (IED) of 5 mm or 10 mm in different sets of simulations, located halfway between the innervation zone and one tendon region. Ten detection systems were placed at the surface of the volume conductor (Figure 1), with centres at a transversal angle in the range 0º - 45º (5° step) with respect to the centre of the muscle (placed at 0º).

Figure 1 about here

Motor unit

The SFAPs were summed together to obtain the MUAPs. Given the location of the centre of a MU and its size N, where N indicates the number of fibres belonging to the MU, the SFAPs corresponding to the N simulated fibres placed closest to the centre of the considered MU were summed to simulate the MUAP. Thus, MUs with circular territory were obtained (possibly deformed in the case of superficial MUs) with centres located randomly within the active muscle (Figure 1). An approximation is introduced by simulating a low density of fibres. This is based on the fact that the same SFAP could be used in the simulation of the MUAPs of overlapping MUs.

The average length of the fibres from the end-plate to the distal and proximal tendon endings was either 30 mm or 50 mm (Table 2). The length of a specific fibre depended on the actual position of the end plate and fibre end, which were randomly chosen (using a uniformly distributed random function) in order to simulate a 10 mm spread of end plate and tendon region. The fibre density within the MU

territory was 20 fibres/mm^2 [29]. The number of fibres per MU was uniformly distributed in the range 50 - 1000 and the total number of simulated MUs was 200. Each MU was assigned a specific conduction velocity (CV). CV distribution was Gaussian with mean 4 m/s and standard deviation 0.3 m/s [31]. CV values were limited in the range 2 - 7 m/s and were assigned in agreement to the size principle, i.e., CV increased with MU size [32].

Motor unit discharge patterns

Eighty percent of maximal voluntary contraction (MVC) was simulated. MUs in the muscle were all active, as recruitment of new MUs ceased at 75% MVC (see Table 1). The MU discharge rate was computed on the basis of the MU recruitment threshold, described by the following function:

$$RTE(i) = RR^{i/n}, \quad i = 1, 2, 3, ..., n \tag{1}$$

where *RTE* indicates the recruitment threshold (in percentage of the maximal force, MVC) of each MU, *RR* denotes the percentage of the maximal force at which all MUs are recruited, *i* is the number denoting the MU, and *n* the total number of MUs in the active muscle [29].

The firing rate of each MU was computed with the following equation:

$$f\_rate(i) = f_{\min} + sl\_dis \cdot (100 - RTE(i)) \tag{2}$$

with f_{min} = 8 pulses per second (pps) corresponding to the minimum firing rate and sl_dis = 0.3 pps/%MVC the variation in discharge rate with force. Discharge rates were thus assigned in inverse order of MU size [15,29,33]. The upper limit of MU firing rate was set to 35 pps.

Inter-pulse interval variability followed a Gaussian distribution with standard deviation equal to 15% of the mean inter-pulse interval. The convolution of the MUAP with the MU firing pattern resulted in the MUAP train detected at the skin surface. Summing the contributions of all MUs in the active muscle resulted in the interference EMG signal.

Simulated signals had a sampling frequency of 4096 Hz and were noise free in order that the perturbation of surface EMG signals as result of only crosstalk could be studied.

Signal analysis

Average rectified value (ARV) and mean power spectral frequency (MNF) were computed from 1 s long simulated signals at the 10 transversal locations for each spatial filter. Ten different distributions of MUs within the muscle were considered for each simulation set. For each transversal location, mean and standard deviation of ARV and MNF, normalized with respect to the average of the values assumed at the first location, were considered. The decrease in ARV with increasing distance from the active muscle provided an indication of selectivity with respect to crosstalk signals. For example, the ARV will decrease rapidly as a function of radial distance from the active muscle with a filter with high selectivity as opposed to filters with lower selectivity where the ARV will decrease slowly as a function of radial distance from the active muscle. MNF gave information on the frequency content of crosstalk signals.

RESULTS

The performance of the monopolar filters has been omitted from some of the results for the sake of clarity. Figure 2 shows sample surface EMG signals and the corresponding power spectra.

Figure 2 about here

Influence of subcutaneous layer thickness

Figure 3 shows ARV and MNF obtained from the simulation with two subcutaneous layer thicknesses.

Figure 3 about here

When the distance between the detection system and the muscle is small, the results obtained by all the detection systems are comparable, but they start to diverge as the distance increases. For a subcutaneous layer thickness of 1 mm, the DD and NDD have comparable selectivity up to approximately 25^{o} after which the most selective filter varies between DD and NDD. SD is the least selective over all the detection points. For a subcutaneous layer thickness of 5 mm, the NDD filter is the most selective over all the detection points, followed by the DD, and then the SD.

MNF of SD, DD and NDD signals initially decrease with increasing transversal distance from the muscle. It then shows a flattening and eventually an increase in value (only in the case of 1 mm fat thickness). The increase is much more evident in NDD than the other two filters. For a subcutaneous layer thickness of 5 mm the MNF decreases less rapidly along the detection points than for a subcutaneous layer thickness of 1 mm and there is no increase in the value of MNF for a subcutaneous layer thickness of 5 mm.

Influence of skin conductivity

The skin conductivity influences the spread of the potentials on the skin surface. Figure 4 shows the results obtained from two simulations with different values of skin conductivity.

Figure 4 about here

From Figure 4 it is clear that an increase in skin conductivity leads to an overall decrease in selectivity. The results obtained with all the detection systems are comparable for small distances between the muscle and detection system. For a skin conductivity of 1 S/m, the NDD filter becomes the most selective as the distance increases, followed by DD, and then SD. When the skin conductivity is decreased, the selectivity of NDD and DD are comparable and equal at some points, varying slightly at greater distances.

MNF again shows a decrease and flattening off as a function of the angular transversal distance from the geometric centre of the muscle. With an increase in skin conductivity, the MNF values do not decrease as rapidly with increasing distance. SD results in the largest decrease in frequency components, followed by DD, then NDD. A decrease in skin conductivity does not change this order.

Effect of IED

The transfer function of a spatial filter depends on IED [1]. Figure 5 shows the results obtained from a simulation using the same library in both cases, but changing the IED from 5 mm to 10 mm.

Figure 5 about here

Changing the IED does not significantly change the order of most selective to least selective filter, implying that the variation in selectivity as the distance around the limb increases is still present with an IED of either 5 or 10 mm, followed by DD and then SD. An increase in IED shows a reduction in the amount by which the MNF is reduced as a function of detection system angle (Figure 5b).

Effect of fibre length

Figure 6 shows the results of a simulation using library 1 with varying fibre length.

Figure 6 about here

From Figure 6a it can be seen that the selectivity of the SD filter increases with increased fibre length. Indeed, end-of-fibre components are more important in the case of short fibres. For the DD and NDD filters, the selectivity is comparable for both fibre lengths (indeed DD and NDD are less affected by end-of-fibre components with respect to SD signals).

Again the variation in the selectivity (among different spatial filters) can be seen for an increase in distance for both fibre lengths. A decrease in fibre length does not influence the order of amplitude selectivity.

For short fibres NDD has the most selective frequency response, followed by DD and then SD. MNF of SD, DD and NDD increases relative to the 0° detection angle when the fibre length decreases. De-normalised data of Figure 6b (not shown here) also suggest that fibre length decrease causes an increase in the absolute value of the MNF. This increase was also observed in simulations performed in [27].

When longer fibres are simulated, NDD again shows the lowest normalised MNF value at first, but SD overtakes it as the distance increases. There is a large increase in frequency components with a decrease in fibre length which can be seen on the de-normalised values (not shown here).

Amplitude of signals detected by different filters for different anatomies

Figure 7 shows the ARV of surface EMG detected by monopolar, SD, DD and NDD filters, normalised with respect to the mean ARV of the monopolar signal detected at angle 0° (average across different simulated subjects). The amplitudes of the signals detected by the different filters can be compared.

All the anatomies described in Table 2 are considered with an IED of 5 mm. The amplitude of the signals is affected by the anatomy and by the location. For example, if subcutaneous tissue is thick, common mode components are large and monopolar signals have large amplitudes with respect to that of the signals detected by other filters which reduce common mode components. In the case of library 4, for detection angles in the range 0°-20°, signals detected by the monopolar system have a maximum ARV with respect to the other filters, which decreases according to the following order: SD, NDD and DD. This order changes for higher angles, for which NDD is the most selective filter. Furthermore, the order changes completely when considering different anatomies. For example, in the case of thin subcutaneous tissue and low skin conductivity (libraries 1 and 5), signals detected using NDD filter have the highest amplitude when detected over the muscle (which extends from detection angles between 0° and 20°, see Figure 1).

Figure 7 about here

DISCUSSION AND CONCLUSION

In surface EMG, spatial selectivity is usually associated with the high-pass cut-off frequency of the detection system [26]. The sources are low-pass filtered by the volume conductor with cut-off frequency inversely related to the distance. Thus, far sources present smaller spatial bandwidth than superficial sources and high-pass spatial filtering reduces their influence on the surface recording. However, the high-pass spatial filtering effect of the detection system applies to signals which propagate along the main direction of the spatial filter. In these cases, space and time domains are related by conduction velocity, which scales the time axis and time-frequency with respect to space and spatial frequency.

For non-travelling components, the relation between the space and time domains by CV does not hold and considering a detection system as a spatial filter is not appropriate. Thus, selectivity with respect to non-travelling components is difficult to predict.

In this study a realistic model for the generation of interference surface EMG signals as recorded during 80% of MVC was applied for comparing spatial filter selectivity with respect to crosstalk. Noise (electrode-skin noise, electronic noise, etc. see [34]) was not simulated. Nevertheless, Figure 7 shows the ARV of the simulated signals normalised with respect to the monopolar signal detected at 0°. Consideration of the contribution of crosstalk with respect to the noise level can be provided, if the amplitude of noise is known. For example, suppose that the noise level is expressed in terms of the maximum amplitude of monopolar signals (which is attained when detection is performed at angle 0°). Suppose that the peak to peak amplitude of the signal is of the order of 400 μV, that of noise is of the order of 4 μV, and a SNR = 40 dB for the monopolar signal. Were the level of noise constant for each detection location and only the amplitude of the signal changed, it can be concluded that the contribution of crosstalk to monopolar signals is over the noise level until the signal amplitude shown in Figure 7 is decreased to 10^{-2} of that recorded at 0°. When a different spatial filter is considered, the amplitudes of the recorded signals and noise change (and as a consequence SNR of different spatial filters is also different). Assuming that noise is spatially uncorrelated (common mode interference such as that coming from a power line is neglected), its amplitude increases proportionally to the number of electrodes and the weights used for the spatial filter. This means that the peak to peak amplitude of the noise of SD, DD, NDD is 2-, 4-, 8-times larger than that recorded by a monopolar channel, respectively. Thus, in the case of SD, DD, NDD the contribution of crosstalk is over the noise level until the signal amplitude shown in Figure 7 is decreased to $2 \cdot 10^{-2}$, $4 \cdot 10^{-2}$, $8 \cdot 10^{-2}$, respectively. Thus, the results provided in Figures 3-6 for low amplitudes of the signal could not be obtained in real

experiments when the amplitude decay for monopolar, SD, DD, NDD is about 100-fold, 50-fold, 25-fold, 12-fold lower, respectively, with respect to that of a monopolar signal recorded directly over the active muscle, as the EMG (crosstalk) signals would be hidden by noise.

In a previous study [27], we analysed the effect of the spatial filter and of the volume conductor on single fibre recordings. These results suggested that selectivity with respect to crosstalk rejection depends on the volume conductor model considered. Interference EMG signals were simulated in this paper. Some of the indications provided in the previous work based on SFAPs are still valid. Indeed, the anatomy and physical parameters selected for the simulations have important effects on the selectivity of different filters. The NDD filter and the DD filter are more selective than monopolar and SD filters in most of the cases. Nevertheless, the effect of the volume conductor on the performance of the filters prevents the possibility of selecting an optimal spatial filter which is subject-independent. For example, one of the parameters which largely affect the selectivity of the filter is skin conductivity. This is a parameter difficult to measure, as it is affected by many external factors (such as humidity, stress, sweat, etc.).

Generally, NDD is more selective closer to the source and DD more selective further from the source. This result indicates that an isotropic filter with a large number of electrodes like NDD can be very selective to propagating components, i.e. near field potentials, and an anisotropic filter with a smaller number of electrodes like DD can be very selective with respect to end of fibre components, i.e. far field potentials. Nevertheless, the selectivity cannot be accurately predicted without considering the actual volume conductor under consideration. Increasing the subcutaneous layer and skin conductivity, favourably affected the NDD filter.

Considering shorter fibre lengths the relative contribution of end-of-fibre components with respect to travelling components increases. Selectivity of SD filter (which is more affected by end-of-fibre

components than both DD and NDD) is lower when shorter fibres are considered. On the other hand, the selectivity of the NDD and DD filters was not affected by fibre length.

Increasing IED decreased the selectivity of all the filters by only a small amount. It was found that the largest decrease in selectivity was present with the NDD filter. This indicates that NDD filters are more sensitive to changes in IED than the SD and DD filters which is probably due to the larger spatial dependence of NDD filters.

It is worth noting that the simulated volume conductor was very simple. The effect of the actual volume conductor (i.e., a portion of human body) on selectivity of different detection systems may be more important when experimental signals are considered. For example, when a more complicated volume conductor is considered, even in simulations as in [35], more selective filters can be significantly affected by local in-homogeneities.

Thus, the main finding of this paper is that the spatial filter which is optimal in terms of crosstalk reduction largely depends on anatomy and specifically on fat thickness and skin conductivity. This merely introduces limitations in the application of models in designing optimal spatial filters. This suggests that methods need to be developed to select the optimal detection technique on the basis of the specific signal which is considered. Adaptive methods to process EMG signals have been recently developed for other purposes (e.g. the compression of the signal [36] or the blind separation of the signals from different muscles [37], which could ideally remove crosstalk from the recorded signals). The development of signal-based methods to select the optimal spatial filter to obtain signals with minimum content of crosstalk is suggested. This would require a quantitative measure of crosstalk (still not available in the literature) in order to select the optimal detection configuration. The use of models will be valuable for these possible future perspectives.

ACKNOWLEDGEMENTS

This work is supported by the Italian-South African Research Collaboration Programme under the project "Neuromuscular system assessment by surface EMG: finite element modelling" and by the European Community Project CyberManS (Cybernetic Manufacturing Systems) number 016712. The authors are grateful to Prof. R. Merletti and Prof. D. Farina for their supervision.

REFERENCES

[1] Farina D, Merletti R, Indino T, Graven-Nielsen T. Surface EMG crosstalk evaluated from experimental recordings and simulated signals. Reflections on crosstalk interpretation, quantification and reduction, Methods of Information in Medicine, 2004; 43: 30-35.

[2] Koh TJ, Grabiner MD. Cross talk in surface electromyograms of human hamstring muscles, Journal of Orthopaedic Research, 1992; 10: 701-709.

[3] Dimitrov GV, Disselhorst-Klug C, Dimitrova NA, Schulte E, Rau G. Simulation analysis of the ability of different types of multi-electrodes to increase selectivity of detection and to reduce crosstalk, J Electromyogr Kinesiol, 2003; 13: 125-138.

[4] De Luca CJ, Merletti R. Surface myoelectric signal cross-talk among muscles of the leg", Electroencephalography and clinical Neurophysiology, 1988; 69: 568-575.

[5] Merletti R., Parker P.A. (editors), Electromyography: Physiology, engineering and non invasive applications, IEEE Press / J Wiley, USA, 2004.

[6] Morrenhof JW, Abbink HJ. Cross-correlation and cross-talk in surface electromyography, Electromyography and Clinical Neurophysiology, 1985; 25: 73-79.

[7] Farina D, Cescon C, Merletti R. Influence of anatomical, physical and detection-system parameters on surface EMG", Biological Cybernetics, 2002; 86: 445-456.

[8] van Vugt JPP, van Dijk JG. A convenient method to reduce crosstalk in surface EMG, Clinical Neurophysiology, 2000; 112: 583-592.

[9] Mogk JPM, Keir PJ. Crosstalk in surface electromyography of the proximal forearm during gripping tasks, J Electromyogr Kinesiol, 2003; 13: 63-71.

[10] Dimitrova NA, Dimitrov GV, Nikitin OA. Neither high-pass filtering nor mathematical differentiation of the EMG signals can considerably reduce cross-talk, J Electromyogr Kinesiol, 2002; 12: 235-246.

[11] Lowery MM, Stoykov NS, Kuiken TA. A simulation study to examine the use of cross-correlation as an estimate of surface EMG cross talk, Journal of Applied Physiology, 2003; 94: 1324-1334.

[12] Farina D, Rainoldi A. Compensation of the effect of sub-cutaneous tissue layers on surface EMG: a simulation study, Medical Engineering and Physics, 1999; 21: 487-496.

[13] Stegeman DF, Dumitru D, King JC, Roeleveld K. Near- and Far-Fields: Source Characteristics and the Conducting Medium in Neurophysiology, American Clinical Neurophysiology Society, 1997; 14 (5): 429-442.

[14] Farina D, Merletti R, Indino B, Nazzaro M, Pozzo M. Surface EMG crosstalk between knee extensor muscles: experimental and model results, Muscle & Nerve, 2002; 26: 681-695.

[15] Basmajian JV, De Luca CJ. Muscles Alive: Their function revealed by electromyography. 5 Baltimore: Williams & Williams, 1985.

[16] Lindstrom LH, Magnusson RI. Interpretation of myoelectric power spectra: a model and its applications, Proceedings of the IEEE, 1977; 65 (5): 653-662.

[17] Roeleveld K, Blok JH, Stegeman DF, van Oosterom A. Volume conduction models for surface EMG: confrontation with measurements, J Electromyogr Kinesiol, 1997; 7 (4): 221-232.

[18] Solomonow M, Baratta R, Bernardi M, Zhou B, Lu Y, Zhu M, Acierno S. Surface and wire EMG crosstalk in neighbouring muscles, J Electromyogr Kinesiol, 1994; 4: 131-142.

[19] Lowery MM, Stoykov NS, Taflove A, Kuiken TA. A multiple-layer finite-element model of the surface EMG signal, IEEE Trans. Biomed. Eng., 2002; 49 (5): 446-54.

[20] Mesin L. Simulation of Surface EMG Signals for a Multi-layer Volume Conductor with a Superficial Bone or Blood Vessel, IEEE Trans. Biomed. Eng., in press, 2008.

[21] Lowery MM, Stoykov NS, Kuiken TA. Independence of myoelectric control signals examined using a surface EMG model, IEEE Trans. Biomed. Eng., 2003; 50 (6): 789-793.

[22] Broman H, Bilotto G, De Luca CJ. A note on the noninvasive estimation of muscle fiber conduction velocity, IEEE Trans. Biomed. Eng., 1985; 32: 341-344.

[23] Reucher H, Silny, J, Rau G. Spatial filtering of noninvasive multielectrode EMG: part 2 - Filter performance in theory and modeling, IEEE Trans. Biomed. Eng., 1987; 34 (2): 106-113.

[24] Farina D, Cescon C. Concentric-ring electrode system for noninvasive detection of single motor unit activity, IEEE Trans. Biomed. Eng., 2001; 48 (11): 1326-1334.

[25] Farina D, Arendt-Nielsen L, Merletti R, Indino B, Graven-Nielsen T. Selectivity of spatial filters for surface EMG detection from the tibialis anterior muscle, IEEE Trans. Biomed. Eng., 2003; 50 (3): 354-364.

[26] Disselhorst-Klug C, Silny J, Rau G. Improvement of spatial resolution in surface-EMG: A theoretical and experimental comparison of different spatial filters, IEEE Trans. Biomed. Eng., 1997; 44 (7): 567-574.

[27] Farina D, Mesin L, Martina S, Merletti R. Comparison of spatial filter selectivity in surface myoelectric signal detection: influence of the volume conductor model", Med. Biol. Eng. Comp., 2004; 42: 114-120.

[28] Farina D, Mesin L, Marina S, Merletti R. A surface EMG generation model with multilayer cylindrical description of the volume conductor, IEEE Trans. Biomed. Eng., 2004; 51(3): 415-426.

[29] Fuglevand AJ, Winter DA, Patla AE. Models of recruitment and rate coding organization in motor-unit pools, Journal of Neurophysiology, 1993; 70 (6): 2470-2488.

[30] Yamamoto T, Yamamoto Y. Electrical properties of the epidermal stratum corneum, Med. Biol. Eng., 1976; 14: 151-158.

[31] Troni W, Cantello R, Rainero I. Conduction velocity along human muscle fibers in situ, Neurology, 1983; 33 (11): 1453-1459.

[32] Andreassen S, Arendt-Nielsen L. Muscle fibre conduction velocity in motor units of the human anterior tibial muscle: a new size principle parameter, J Physiol., 1987; 391: 561-71.

[33] Stegeman DF, Blok JH, Hermens, HJ, Roeleveld, K. Surface EMG models: properties and applications, J Electromyogr Kinesiol, 2000; 10: 313-326.

[34] Clancy EA, Morin EL, Merletti R. Sampling, noise-reduction and amplitude estimation issues in surface electromyography, J Electromyogr Kinesiol, 2002; 12: 1-16.

[35] Mesin L, Farina D. A model for surface EMG generation in volume conductors with spherical inhomogeneities, IEEE Trans. Biomed. Eng., 2005; 52: 1984-93.

[36] Brechet L, Lucas MF, Doncarli C, Farina D. Compression of biomedical signals with mother wavelet optimization and best-basis wavelet packet selection. IEEE Trans Biomed Eng., 2007; 54: 2186-2192.

[37] Farina D, Lucas MF, Doncarli C. Optimized wavelets for blind separation of nonstationary surface myoelectric signals. IEEE Trans Biomed Eng. 2008; 55: 78-86.

TABLE CAPTIONS

Table 1. Fixed model parameter used for the simulations.

Table 2. Parameters of the six anatomical libraries investigated.

FIGURE CAPTIONS

Figure 1. The model of the limb with bone, muscle, subcutaneous tissue, and skin layers. Ten locations were selected for the centres of the detection systems. Figure 1(a) shows the anatomy used for libraries 1,2 and 5 of Table 2 and figure 2(b) shows the anatomy used for libraries 3,4 and 6. The semi-axes of the ellipse shown are r1 = 11.5 mm and r2 = 16 mm.

Figure 2. Representative simulated EMG signal and power spectra as detected with three detection systems at 0 º, 20 º and 45 º. Subcutaneous layer = 1 mm, skin conductivity = 0.02 S/m, fibre length = 50 mm, IED = 5 mm. The mean frequency values are indicated by the dotted lines on the power spectra graphs. Detection systems used are single differential (SD), double differential (DD) and normal double differential (NDD).

Figure 3. ARV (a) and MNF (b) of library 1 (filled markers, subcutaneous layer = 1 mm) and library 3 of Table 2 (unfilled markers, subcutaneous layer = 5 mm). The circles represent the NDD filter, the squares represent the DD filter and the diamonds represent the SD filter. Skin conductivity = 0.02 S/m, fibre length = 50 mm, IED = 5 mm. The values display the mean of 10 averages with the standard deviations indicated.

Figure 4. ARV (a) and MNF (b) corresponding to library 1 (filled markers, conductivity = 0.02 S/m) and library 2 of Table 2 (unfilled markers, skin conductivity = 1 S/m). The circles represent the NDD filter, the squares represent the DD filter and the diamonds represent the SD filter. IED = 5 mm, fibre length = 50 mm, subcutaneous layer = 1mm.

Figure 5. ARV (a) and MNF (b) for library 1 of Table 2 with IED = 5 mm (filled markers) and IED = 10 mm (unfilled markers). The circles represent the NDD filter, the squares represent the DD filter and the diamonds represent the SD filter. Fiber length = 50 mm, subcutaneous layer = 1mm, skin conductivity = 0.02 S/m.

Figure 6. ARV (a) and MNF (b) of library 1 (filled markers, fibre length = 50 mm) and library 5 of Table 2 (unfilled markers, fibre length = 30 mm). The circles represent the NDD filter, the squares represent the DD filter and the diamonds represent the SD filter. IED = 5 mm, subcutaneous layer = 1mm, skin conductivity = 0.02 S/m.

Figure 7. ARV of monopolar, SD, DD and NND filters normalised with respect to the mean value of ARV (average across different subjects) of monopolar signals at 0° of library 1 to 6 of Table 2 with IED values of 5 mm in all cases. The circles represent the NDD filter, the squares represent the DD filter, the diamonds represent the SD filter and the triangles represent the monopolar filter. The values display the mean of 10 averages with the standard deviations indicated.

Table 1. Fixed model parameter used for the simulations.

Parameter	**Value**
Limb radius	50 mm
Bone radius	20 mm
Skin thickness	1 mm
Fibers / MU (uniform distribution of MU size)	50 – 1000
MU / muscle	200
Simulated fibre density	20 fibres/mm²
Conductivity of bone (isotropic)	0.02 S/m
Conductivity of subcutaneous layer (isotropic)	0.05 S/m
Conductivity of muscle (radial + angular)	0.1 S/m
Conductivity of muscle (longitudinal)	0.5 S/m
Inter-electrode distance (IED)	5 mm
Physiologic cross-sectional area (PCSA) of selected muscle	600 mm²
Muscle horizontal semi-axis	16 mm
Muscle vertical semi-axis	11.5 mm
Maximum force exerted by muscle	100 % MVC
% MVC where recruitment stops (RR)	75%
Interpulse interval variability	15%
Variation in discharge rate with force (*sl_dis*)	15%
Simulated force (%MVC)	80%

Table 2. Parameters of the six anatomical libraries investigated.

Library number	Skin conductivity (S/m)	Subcutaneous layer thickness (mm)	Fibre semi-length (mm)
1	0.02	1	50
2	1	1	50
3	0.02	5	50
4	1	5	50
5	0.02	1	30
6	0.02	5	30

Fig 1

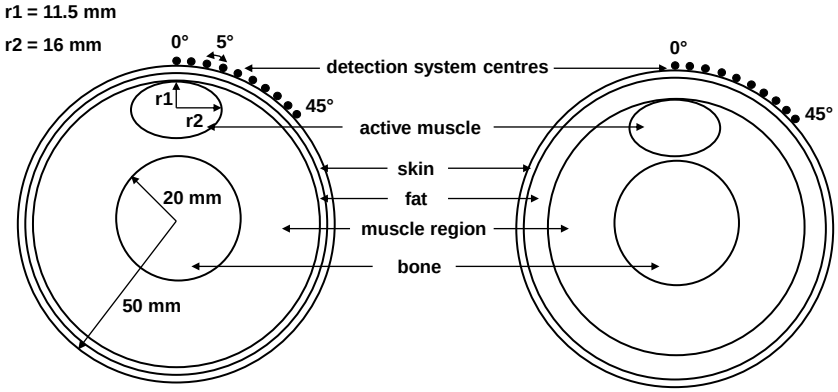

Libraries 1, 2 and 5 **Libraries 3, 4 and 6**

Fig 2

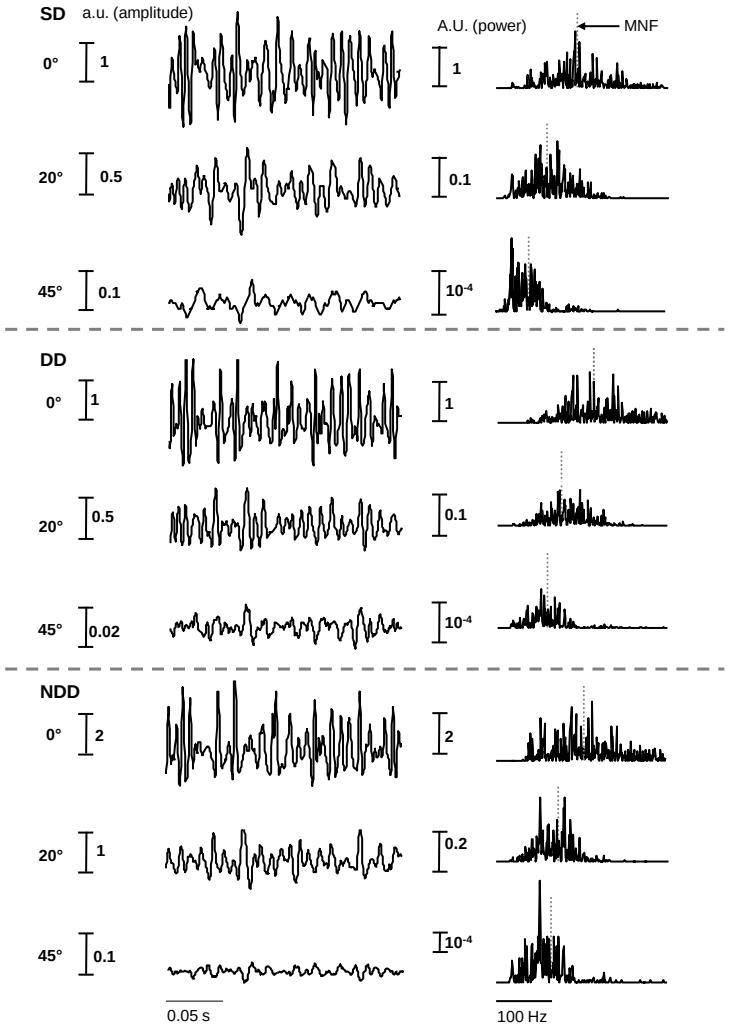
SD
a.u. (amplitude)
A.U. (power)
MNF
0°
1
1
20°
0.5
0.1
45°
0.1
10-4
DD
0°
1
1
20°
0.5
0.1
45°
0.02
10-4
NDD
0°
2
2
20°
1
0.2
45°
0.1
10-4
0.05 s
100 Hz

Fig 3

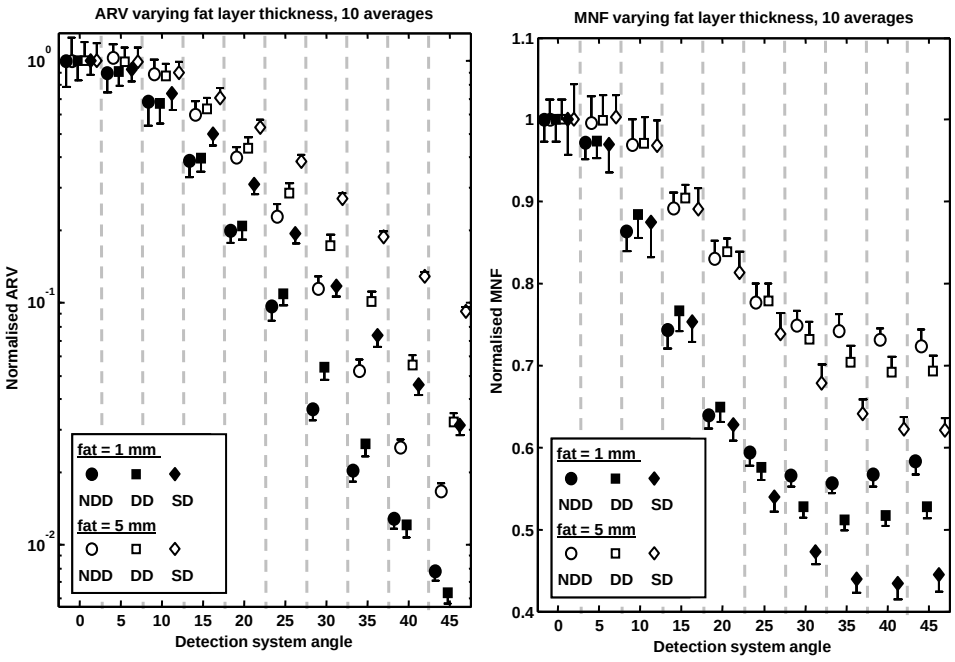
ARV varying fat layer thickness, 10 averages
Normalised ARV
Detection system angle
fat = 1 mm
NDD DD SD
fat = 5 mm
NDD DD SD
MNF varying fat layer thickness, 10 averages
Normalised MNF
Detection system angle
fat = 1 mm
NDD DD SD
fat = 5 mm
NDD DD SD

Fig 4

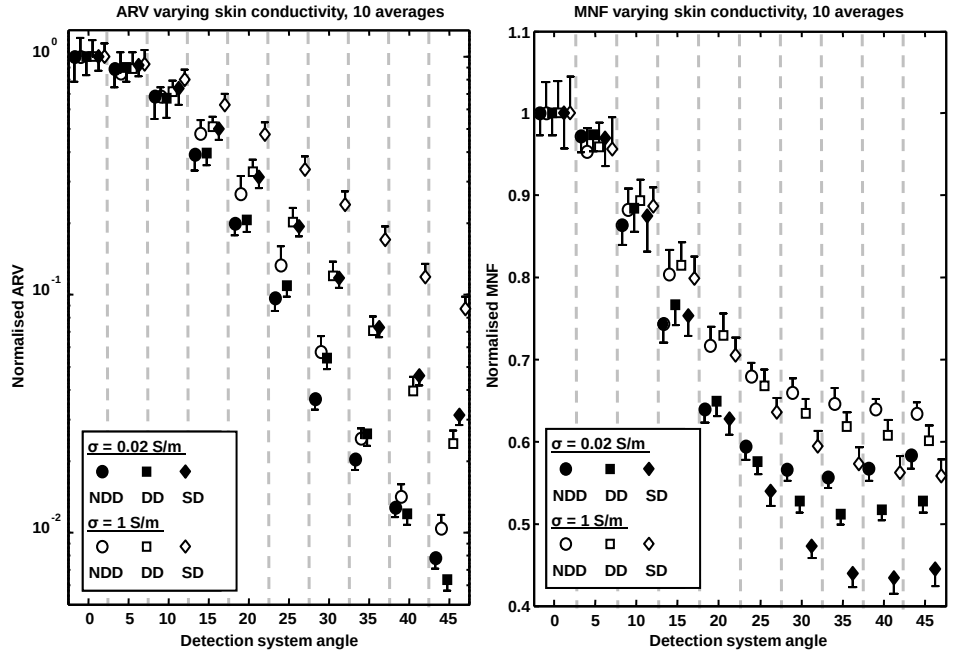
ARV varying skin conductivity, 10 averages
Normalised ARV
Detection system angle
σ = 0.02 S/m
NDD DD SD
σ = 1 S/m
NDD DD SD
MNF varying skin conductivity, 10 averages
Normalised MNF
Detection system angle
σ = 0.02 S/m
NDD DD SD
σ = 1 S/m
NDD DD SD

Fig 5

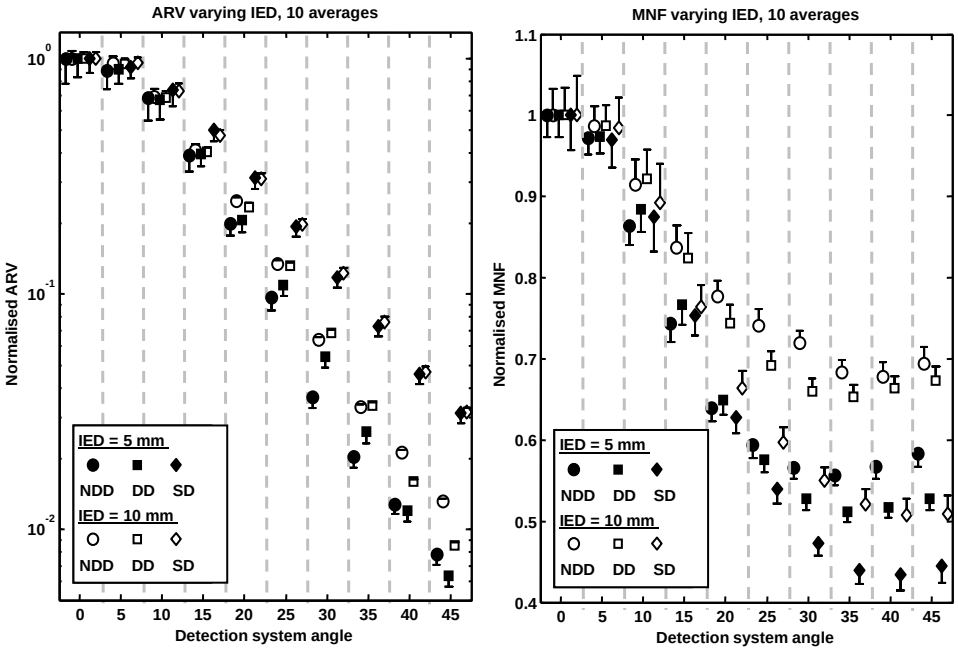
ARV varying IED, 10 averages
Normalised ARV
Detection system angle
IED = 5 mm
NDD DD SD
IED = 10 mm
NDD DD SD
MNF varying IED, 10 averages
Normalised MNF
Detection system angle
IED = 5 mm
NDD DD SD
IED = 10 mm
NDD DD SD

Fig 6

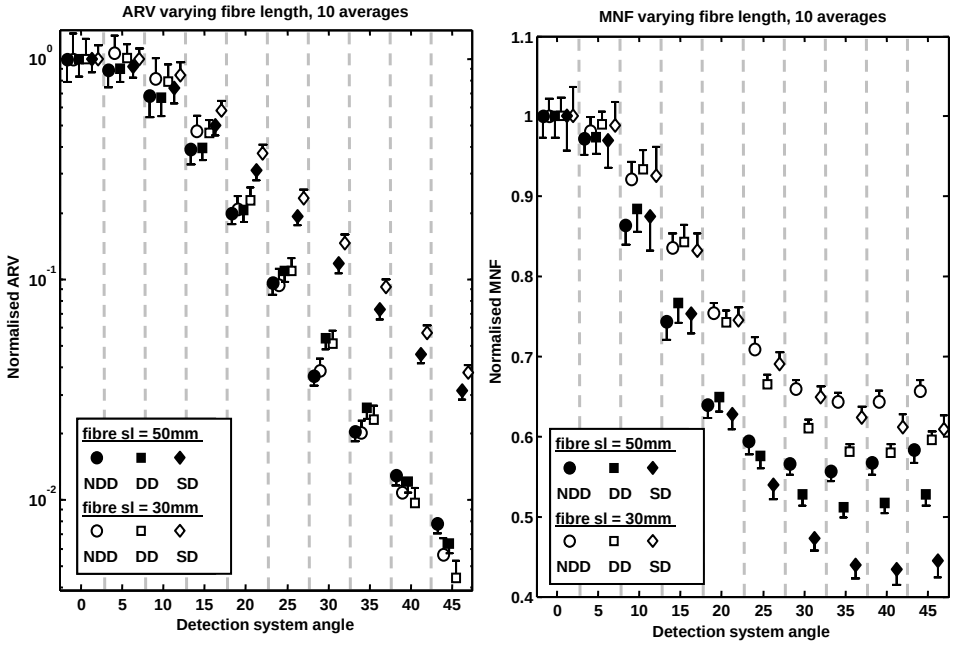
ARV varying fibre length, 10 averages
Normalised ARV
Detection system angle
fibre sl = 50mm
NDD DD SD
fibre sl = 30mm
NDD DD SD
MNF varying fibre length, 10 averages
Normalised MNF
Detection system angle
fibre sl = 50mm
NDD DD SD
fibre sl = 30mm
NDD DD SD

Fig 7

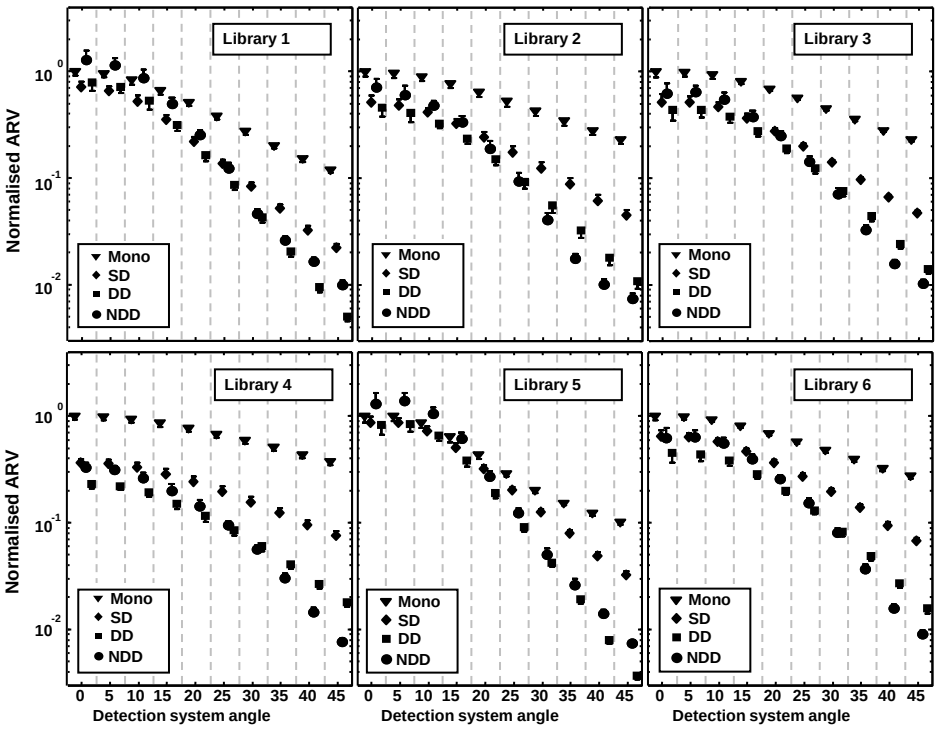
Library 1
Library 2
Library 3
Library 4
Library 5
Library 6
Mono
SD
DD
NDD
Normalised ARV
Detection system angle